# Fractal Characterization of Hyperspectral Imagery

**Hong-lie Qiu, Nina Siu-Ngan Lam, Dale A. Quattrochi, and John A. Gamon**

## Abstract

*Two AVIRIS hyperspectral images selected from the Los Angeles area, one representing urban and the other rural, were used to examine their spatial complexity across their entire spectrum of the remote sensing data. Using the ICAMS (Image Characterization And Modeling System) software, we computed the fractal dimension values using the isarithm and triangular prism methods for all 224 bands in the two AVIRIS scenes. The resultant fractal dimensions reflect changes in image complexity across the spectral range of the hyperspectral images. Both the isarithm and triangular prism methods detect unusually high* D *values on the spectral bands that fall within the atmospheric absorption and scattering zones where signal-to-noise ratios are low. Fractal dimensions for the urban area resulted in higher values than for the rural landscape, and the differences between the resulting* D *values are more distinct in the visible bands. The triangular prism method is sensitive to a few random speckles in the images, leading to a lower dimensionality. On the contrary, the isarithm method will ignore the speckles and focus on the major variation dominating the surface, thus resulting in a higher dimension. It is seen where the fractal curves plotted for the entire bandwidth range of the hyperspectral images could be used to distinguish landscape types as well as for screening noisy bands.*

## Introduction

Scientists have been attracted to the scale-independent nature of fractal geometry since the first introduction of fractal theory by Mandelbrot in 1975 (Mandelbrot, 1975). This is especially true for Earth scientists who observe and study landscape features and the associated processes at various scales. The improving spatial resolution of satellite imagery has made it possible to reveal landscape features at finer scales, and scientists are challenged by the need to extend their knowledge from one scale to another. At the same time, new developments in hyperspectral imaging technology have allowed scientists to study landscape features at a much wider spectral range with finer spectral resolutions. While the main use of this newly available hyperspectral imagery is for pixel-based spectral analysis of surface features, images of the individual spectral bands can also be used for mapping and landscape studies. For this type of application, one faces the problem of selecting from hundreds of spectral bands the most suitable one to use and display. An understanding of how image content changes across the spectral bands is necessary, and a reliable quantitative measure capable of describing image content is highly desirable to aid in the interpretation and analysis of these data.

The fractal dimension ($D$) has been used as a spatial measure for describing the complexity of spatial data, including remote sensing imagery (Lam, 1990; Lam and De Cola, 1993). The fractal dimension of a linear feature such as a coastline can be any value between 1 and 2, depending on its complexity. Similarly, for a surface, the fractal dimension value lies between 2 and 3. This dimension value is derived from the entire surface, and it reflects the overall characteristics of the surface. When applied to remote sensing data, an image will be represented as a surface and the fractal dimension value of that surface represents the complexity of the image. In this paper this spatial measure was used to quantify how one image differs from the others in terms of spatial complexity. Specifically, when applied to the narrow-band hyperspectral imagery from AVIRIS (Airborne Visible Infra-Red Imaging Spectrometer), could this single spatial index reflect variations in image content across the spectrum of the scene? Previous studies have shown that fractal dimension ($D$) changes across the spectral bands of Landsat TM imagery (De Cola, 1989; Lam, 1990). However, their conclusions were based on images that have limited spectral resolutions in comparison to that afforded by the AVIRIS sensor. It is useful to examine if similar fractal behavior exists when applied to hyperspectral images, and if fractal dimensions computed for all the bands in the hyperspectral images can be used to reveal the underlying patterns and information content of the landscapes manifested by these images.

In this study we have computed the fractal dimensions for each of the 224 spectral bands available from the AVIRIS for two scenes selected from the Los Angeles region, with one representing an urbanized area and the other a rural area. In addition to examining how fractals behave in hyperspectral images, we investigate how fractals can be used to distinguish landscape types, as manifested in hyperspectral images, by contrasting their computed fractal dimensions across the entire AVIRIS spectral bandwidth range. We also examine the relationship between fractal dimension and im-

H.-L. Qiu is with the Department of Geography and Urban Analysis, California State University, Los Angeles, Los Angeles, CA 90032.

N.S.-N. Lam is with the Department of Geography and Anthropology, Louisiana State University, Baton Rouge, LA 70803.

D.A. Quattrochi is with the National Aeronautics and Space Administration, Global Hydrology and Climate Center, HR20, George C. Marshall Space Flight Center, Marshall Space Flight Center, AL 35812.

J.A. Gamon is with the Department of Biology and Microbiology, California State University, Los Angeles, Los Angeles, CA 90032.

Photogrammetric Engineering & Remote Sensing, Vol. 65, No. 1, January 1999, pp. 63–71.

0099-1112/99/6501–0063$3.00/0

age content (i.e., the data "complexity" of the image as it relates to landscape characteristics and, thus, image content) contained in individual spectral bands. If such a relationship exists, it may be possible to use fractals for initial screening of hyperspectral imagery and as metadata for selecting those bands that are most applicable for analysis of landscape attributes.

## Hyperspectral Image Data

Hyperspectral imagery portrays a landscape in many narrow spectral bands. The fine spectral resolution in the imagery allows the identification of surface features based on the spectral signatures of individual pixels. The hyperspectral data used in this study were acquired by the AVIRIS instrument developed and operated by the NASA Jet Propulsion Laboratory (JPL). The main purpose of AVIRIS is to identify, measure, and monitor constituents of the Earth's surface and atmosphere for understanding processes related to the global environment and climate change. The AVIRIS imaging system flies onboard a NASA ER-2 airplane at approximately 20 kilometers above sea level and can produce calibrated images of the upwelling spectral radiance in 224 contiguous spectral channels with wavelengths from 0.38 to 2.50 micrometers (Vane *et al.*, 1993). When the data from each detector are plotted on a graph, they yield a spectrum. Comparing the resulting spectrum with those of known surfaces reveals information about the composition of the area being viewed by the instrument. Further information on the instrument can be found on the AVIRIS Web site at **http://makalu.jpl.nasa.gov/**. Each image pixel has a continuous spectrum that can be used to derive information based on the signature of interaction of matter and energy expressed in the spectrum. The high spectral resolution and continuous spectrum of AVIRIS data are necessary for identifying and studying surface features in terms of their physiological or landscape characteristics (e.g., land-cover type, pattern) based on their spectral reflectance. For example, it is possible to derive physiological parameters of ground vegetation from the AVIRIS reflectance data (Gamon and Qiu, in press). Experimental studies on the ground at the leaf-to-stand scale have indicated that several narrow-band spectral features can be used to detect plant physiological status (Penuelas and Filella, 1998). However, current knowledge of these processes in plants and vegetation is largely based on studies at small landscape scales and is limited to the ground data (Jarvis, 1995). The real challenge is to be able to "upscale" our existing knowledge to the landscape level using remotely sensed data. For this study, we focus on evaluating the spatial characters of individual images and how they differ according to different landscape types. The hyperspectral nature of the AVIRIS data provides a unique opportunity for testing the sensitivity and applicability of fractal dimension as a spatial index.

Two AVIRIS scenes from the Los Angeles region were selected for this study (Figures 1 and 2). A complete AVIRIS scene covers an area of 10.5 by 8.7 kilometers and is about 140 megabytes in file size. There are a total of 224 spectral bands in an AVIRIS scene; each spectral band consists of 614 by 512 pixels with a 17-meter pixel size. Both AVIRIS scenes were acquired on 23 October 1996, two days after the Calabasas/Malibu brush fire that scarred the Los Angeles study area. The first scene (961023B0501) covers the mountain areas near Malibu located on the southern California coast just west of Los Angeles. The eastern third of the scene has been burned and is marked by a darker tone in Figure 1. The rest of the scene is covered by California chaparral. Because the image was acquired in the middle of the dry season, most of the vegetation is under drought stress conditions. The second AVIRIS scene (961023B0301) covers an urbanized area immediately north of downtown Los Angeles. Compared to the rural scene, this scene has a diversity of land covers, containing vegetation, mixed urban, highway, and others typical of a city landscape. No atmospheric correction has been applied to the two AVIRIS scenes, but we anticipate the lack of atmospheric correction will not create spurious results for this analysis.

A GIS software module called ICAMS (Image Characterization And Modeling System) was used to compute the fractal dimension values of all spectral bands of the two selected AVIRIS scenes. The software module provides three different methods for computing the fractal dimensions of image data: isarithm, triangular prism, and variogram methods (see Lam *et al.* (1997), Quattrochi *et al.* (1997), and Lam *et al.* (1998) for details). Among the three methods, the isarithm method appears to be more stable and robust, but it requires several input parameters from the user. The triangular prism method requires only one user input parameter (i.e., number of measuring steps), but it tends to underestimate the spatial complexity of images. The variogram method also requires several input parameters from the user and its result is the least stable, especially for images that have high spatial complexity (high fractal dimensions) (Lam *et al.*, 1997). Only the first two methods were used for computing the fractal dimensions of the AVIRIS scenes. Because the ICAMS software module was originally designed for one-byte-per-pixel images, a conversion from two-byte-per-pixel to one-byte-per-pixel was performed on the two AVIRIS scenes used in this analysis. Images of all spectral bands were scaled linearly to the 0- to 255-pixel range during this conversion. This normalization process is performed to maintain a common base for comparison across the spectral bands. The advantages and disadvantages of this normalization process and its effects on the fractal measurement will be discussed below.

## Isarithm Method versus Triangular Prism Method

In order to compute the fractal dimension, an image is considered a 3D surface, and its complexity is expressed in terms of its variability over space. Similar to a "natural" surface, such as a hilly terrain or flat plain, this complexity is a function of its vertical variability of pixel values. Hilly terrain has more ups and downs than a flat plain and, thus, represents a more complex surface. This surface complexity can be expressed quantitatively by the fractal dimension $D$. A featureless surface with no measurable complexity would yield a fractal dimension close to 2.0. An infinitely variable or complex surface would result in a fractal dimension close to 3.0. A topographic surface will have a dimension of around 2.2 to 2.3 (Mandelbrot, 1983). Dimension values for image surfaces have been reported to be much higher, and, depending on the types of landscapes examined, they can be as high as 2.7 to 2.9 (Lam, 1990; Jaggi *et al.*, 1993).

The isarithm method has been used frequently for estimating the fractal dimension of image data. This method follows the walking-divider logic by measuring the dimensions of individual isarithms (i.e., iso-spectral reflectance curves) derived from the image surface (Lam and De Cola, 1993; Jaggi *et al.*, 1993). In order to compute the fractal dimension value of an isarithm, the image is divided into two regions — one above the current isarithm and the other below the current isarithm. The length of the isarithm is represented by the number of boundary pixels between the two regions. These boundary pixels are counted at various step sizes. The logarithm of the number of boundary pixels is then regressed against the logarithm of the step size, and the fractal dimension of the isarithm line is calculated based on the slope of the regression. The final dimension of the image is computed by averaging the $D$ values of the isarithms that have high coefficient of determination ($R^2 > 0.9$).

The second method used in this study for calculating the

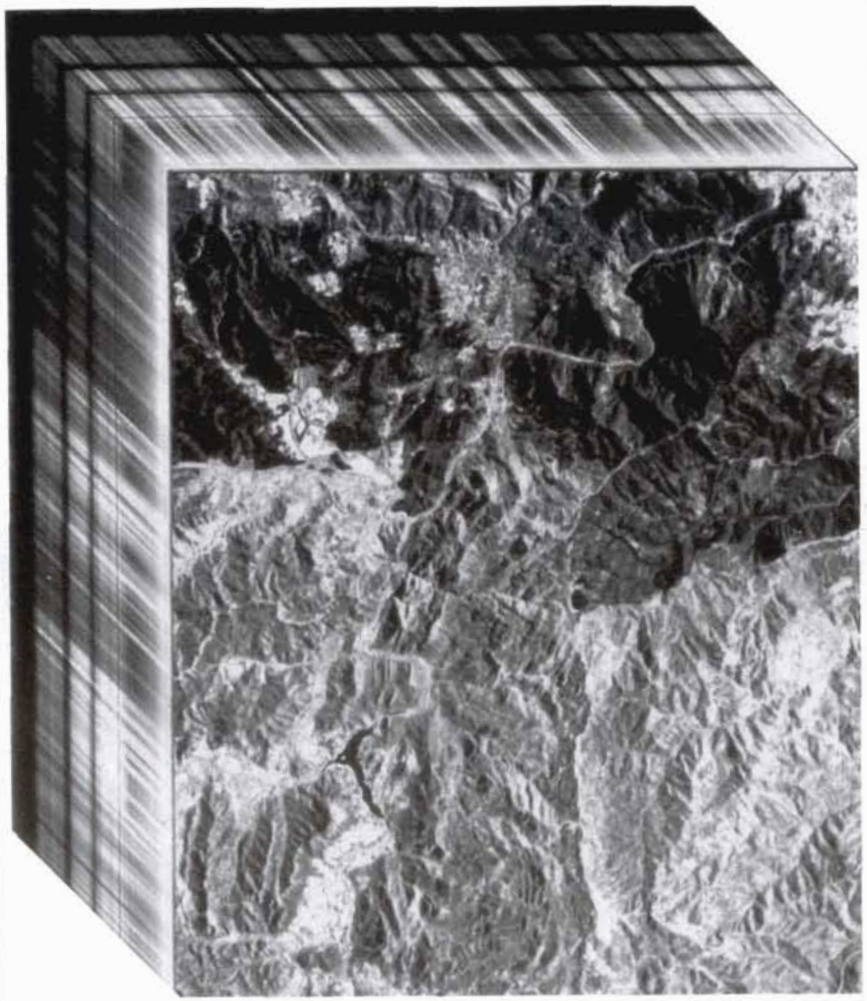

Figure 1. Image data cube derived from the rural AVIRIS scene (961023B0501). The burn scars left by the 1996 Calabasas/Malibu brush fire are found in the eastern one-third of the image. North is to the left.

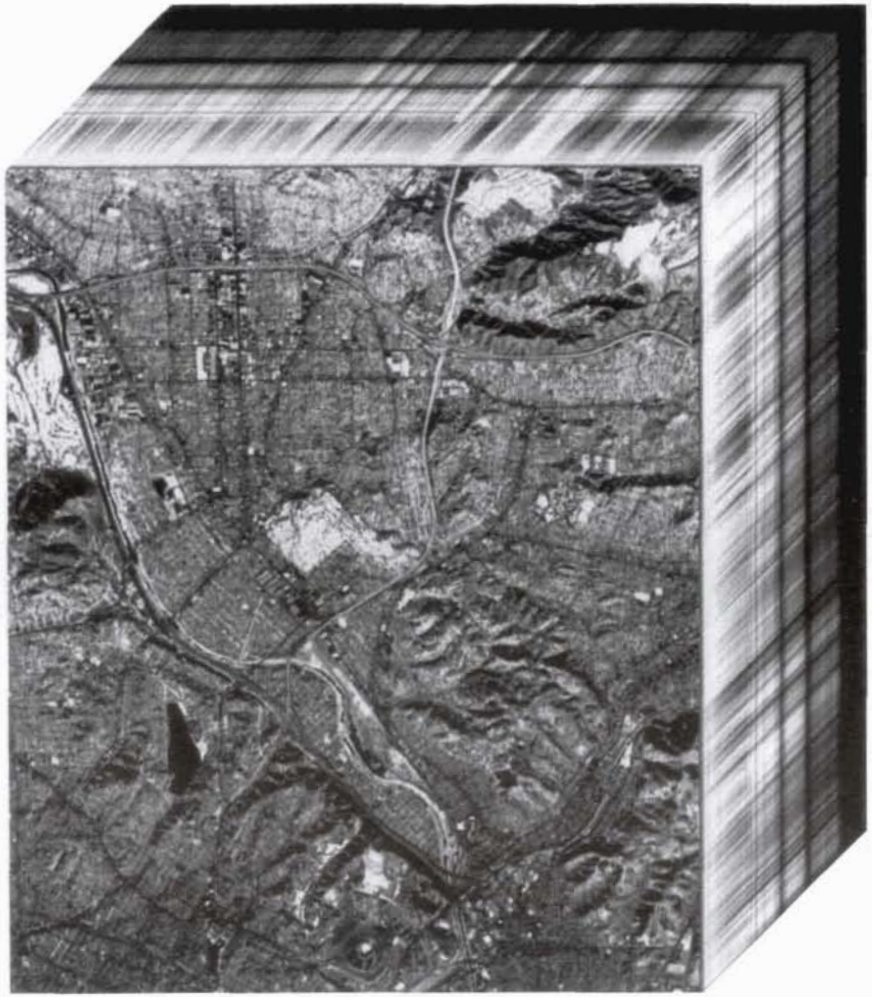

Figure 2. Image data cube derived from the urban AVIRIS scene (961023B0301). Compared to the rural scene, this urban scene has more diverse land-cover types, including vegetation, urban built up areas, transportation systems, and many other features typical of the city landscape. North is to the top.

fractal dimension of an image is the triangular prism method (Clarke, 1986; Jaggi *et al.*, 1993). This algorithm compares the surface areas of triangular prisms using varying sizes of measuring grids on an image surface. This image surface is made up of a series of grids or cells. Each cell is a square whose four corners are represented by the "z" values of the four adjacent pixels. Each pixel value is interpreted as a "z" value, providing a vertical dimension for the cell, and creating a three-dimensional cube. To compute the surface areas, the values of the four pixels are averaged. A vertical line in the center of the cell takes this average as its "z" value. This creates a prism with four triangular facets. The areas of these facets are calculated with a trigonometric formula and then summed to represent the surface area of this particular cell. (See Jaggi *et al.* (1993) for a complete program description and source code in C for the triangular prism method.)

The previous effort calculates the image surface area at its finest step-size resolution. The next task is to compute the image surface area at a coarser step-size resolution using the same triangular prism method. This time, four adjacent cells on the image are considered as a larger composite cell. The four outermost corner or pixel values give this cube its vertical dimension. These values are averaged and a vertical line in the center of this composite cell takes the average as its "z" value. This once again creates a prism with four triangular facets. The areas of these facets are summed to represent the surface area of that composite grid.

The next level considers a composite of 16 cells and the resulting prism facets. Each succeeding computation considers a composite cell area that is exponentially larger than the previous one. With each succeeding measuring unit, the resolution of the image diminishes and information is lost when individual pixel values are replaced with an average in the center. This process can continue until the entire surface area under consideration has been calculated as a single composite cell.

The logarithm of the total surface areas (i.e., sum of all prism facet areas) computed using different measuring resolutions are plotted against the logarithm of the measuring units (i.e., number of cells). The fractal dimension is then calculated by performing a regression on these two variables and inputting the resulting slope of the regression in the equation $D = 2.0 - B$, where $B$ is the slope of the regression. Because $B$ is expected to be of negative value (total surface areas measured decrease with increasing step size), the resultant $D$ should range between 2.0 and 3.0.

It has been reported that the triangular prism method introduced by Clarke (1986) tends to underestimate the fractal dimension of image surface (Jaggi *et al.*, 1993; Lam *et al.*, 1997). A minor modification was introduced in ICAMS in order to improve the performance of the method. We used the number of measuring grids (e.g., 1, 2, 4, 8, 16), instead of the square of the number of measuring grids (e.g., 1, 4, 16, 64, 256) in the regression for dimension computation. This modification results in doubling the value of the regression slope and, consequently, defined a higher, but more accurate, dimension value.

## Results

The basic summary statistics (minimum, maximum, and standard deviation) for individual spectral bands of the two AVIRIS scenes were computed and plotted (Figures 3a and 3b). These summary statistics provide insight about individual bands of the images, but none of them provides information about the spatial variation. The two statistics graphs show several features in common with the two AVIRIS scenes. All four statistics (i.e., maximum and minimum values for each of the AVIRIS scenes) decline to almost zero around band 110 and band 160, the two wavelength regions where water vapor in the atmosphere absorbs almost all of the reflected energy. When the two charts are compared, the urban scene generally has higher maximum pixel values for the first 40 bands, whereas the rural scene has higher maximum pixel values for the last 40 bands. Standard deviation measures the dispersion of pixel values around the mean and can provide some insight into the data distribution, but it is inadequate for describing the spatial variation of image surfaces. Standard deviations of the two images are very similar.

Figure 4 contrasts the two AVIRIS scenes in terms of their coefficients of variation. This statistic is calculated by dividing standard deviation with the mean (i.e., standard deviation/mean) and provides a relative measure on the dispersion of pixel values around its mean. The higher the coefficient of variation, the greater the relative dispersion of pixel values. Figure 4 clearly shows that the rural scene has higher coefficients of variation for most of the spectral bands, suggesting a greater degree of dispersion of pixel values. This statistic, however, suffers the same limitation as does standard deviation: the spatial component of the variation is not measured.

Fractal dimension values for all 224 bands of the two AVIRIS scenes were computed by ICAMS using the isarithm and triangular prism methods. A step size of 5 was used in both methods and a contour interval of 10 was used in the isarithm method. The results are presented in Figures 5a and 5b for each method. Three bands of AVIRIS data (urban band 86, rural band 112, and rural band 195) have incomplete data, and, therefore, fractal dimension values for these bands were not computed.

The most striking feature revealed by both methods is the occurrence of four regions of very high fractal dimension values, shown as spikes on all four curves. Unusually high $D$ values ($D > 2.9$) are found around bands 2, 111, 160, and 221 (0.4, 1.40, 1.85, and 2.4 μm, respectively). Three of the four high fractal dimension regions (1.40, 1.85, and 2.4 μm) correspond well to the three atmospheric absorption zones for water and, therefore, have low signal-to-noise ratios. They have high fractal dimension values because images with low signal-to-noise ratios tend to be highly variable, which elevates $D$ values. The high fractal dimension region near the short wavelength region (0.4 μm) is probably caused by the low solar irradiance and low optical system transmittance at this wavelength (Vane *et al.*, 1993).

Another feature revealed by both fractal measurement methods is that the urban scene yields higher $D$ values than does the rural scene. Based on the fractal dimension values, we delineate the dimension curves into four zones (I to IV) in both figures to facilitate interpretation and discussion. Zone I includes bands 1 to 37 (0.380 to 0.707 μm) and contains approximately all the AVIRIS visible bands. Zone II includes bands 41 to 170 (0.707 to 1.975 μm), encompassing most of the reflected infrared spectrum. Zone III includes bands in the middle reflective infrared wavelengths, 171 to 200 (1.975 to 2.275 μm), as do the bands in zone IV, 201 to 224 (2.275 to 2.513 μm). We caution that these zones are approximate regions and their use is only a device to clarify and facilitate our discussion of the curves presented in Figure 5.

When the fractal values for the urban and rural scenes are compared, a generally greater contrast in dimension values is found in bands within the visible light wavelength region (Zone I), versus a smaller contrast in values in the reflected infrared wavelength region (Zones II and III, except at the problem bands 111 and 160). Outside the visible light wavelength region and especially in Zone II, the dimension curves exhibit less variation and fluctuate around 2.7 (Figures 5a and 5b). A much larger disagreement between the two methods, however, occurs in Zones III and IV (approximately from bands 171 on) of the rural scene. In Zone III (bands 171 to 200), the isarithm method yields fractal dimen-

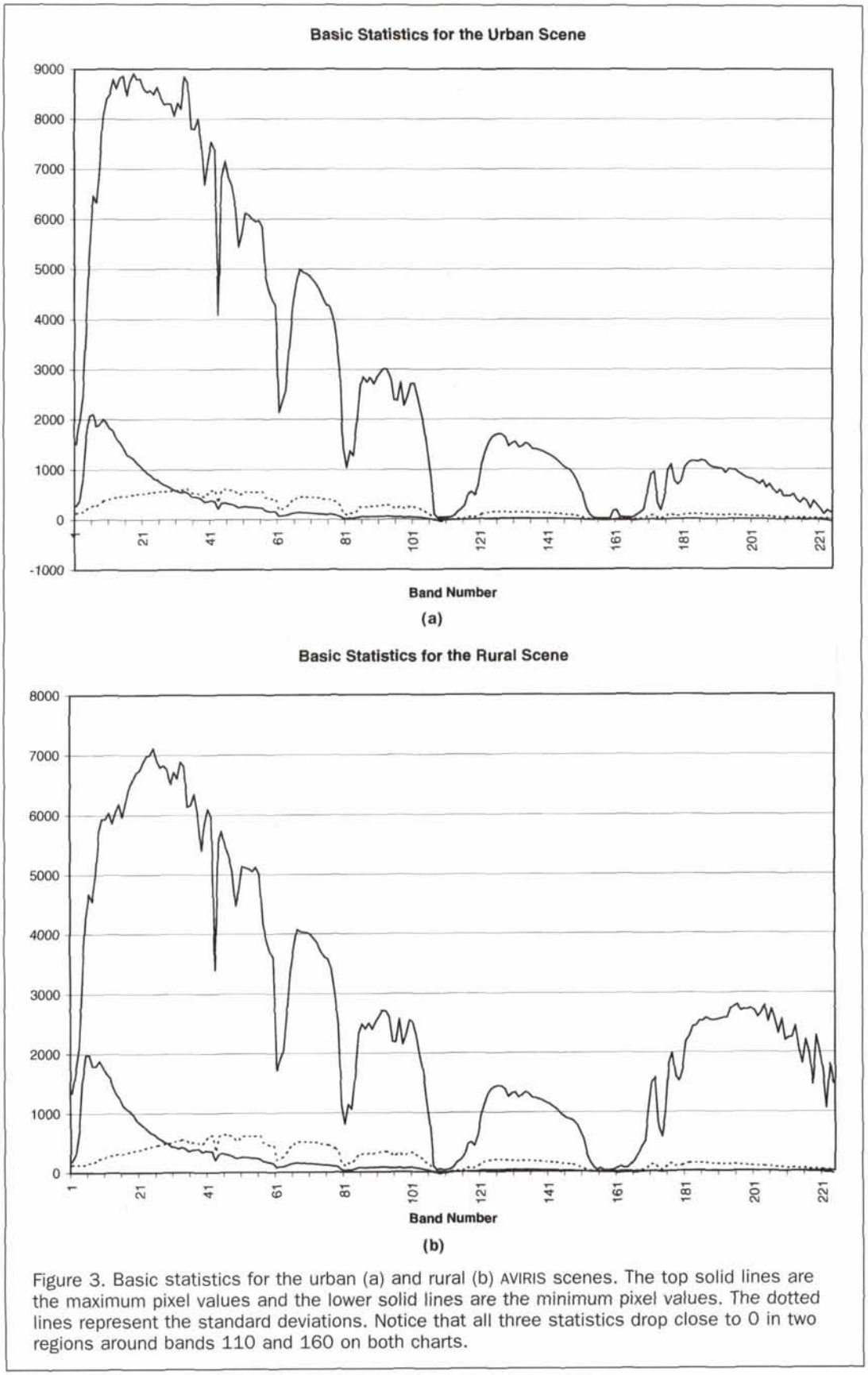


Figure 3. Basic statistics for the urban (a) and rural (b) AVIRIS scenes. The top solid lines are the maximum pixel values and the lower solid lines are the minimum pixel values. The dotted lines represent the standard deviations. Notice that all three statistics drop close to 0 in two regions around bands 110 and 160 on both charts.

sion values similar to those of other reflected infrared bands, and the rural scene has a lower dimension value (around 2.7) than that of the urban scene (2.8). However, at longer wavelengths (Zone IV - bands 201 and up), the pattern reverses and higher dimensions for the rural scene are found instead, though the dimension values as computed by the is-

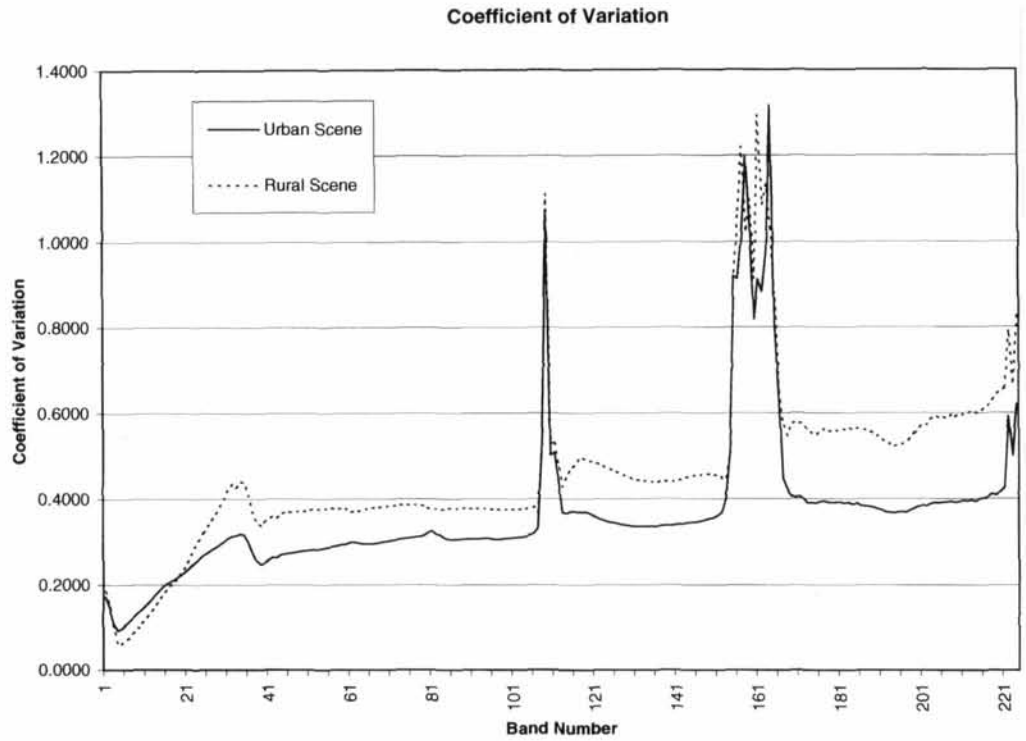


Figure 4. Graph of coefficient of variation by band number for each of two AVIRIS scenes. The rural scene has higher coefficient-of-variation values for most of the spectral bands than does the urban scene. The abrupt increase in coefficient-of-variation values on both scenes is attributed to the low means present in these bandwidth ranges.

arithm method fluctuate greatly in this zone. On the contrary, the triangular prism method yields consistently lower $D$ values over the isarithm method for the rural image, and a distinct declining trend in $D$ values (from 2.6 to 2.4) in Zones III and IV. Such a decline does not appear on the curve generated by the isarithm method for the same scene.

## Discussion

For the AVIRIS data analyzed in this study, unusually high $D$ values ($D > 2.9$) are found in spectral bands where the signal-to-noise ratio is low due to either strong atmospheric absorption or low solar irradiance. Visual inspections of these spectral bands for the two AVIRIS scenes indicate that these bands tend to have poor image content and are dominated by random spectral noise. They resemble fractal dimensions computed for a "white noise" surface that has a dimension value of 3.0. Thus, one practical application resulting from this study is the potential use of fractal dimension as an initial screening tool for identifying the least usable spectral bands, in terms of spectral content, from hyperspectral imagery.

With the isarithm method, the largest contrast between the urban and rural scenes in terms of the fractal dimension values is found within the visible light wavelength region (Zone I). This corroborates the findings from previous studies (Lam *et al.*, 1998; Quattrochi *et al.*, 1998) that have used fractals for analysis of Landsat TM data. The visible difference between the two landscape types is obvious: the urban scene contains many different land-cover types whereas the rural scene has a more uniform land cover (Figures 1 and 2) which affects $D$ values, particularly within the visible portion of the spectrum. Urban scene bands have dimension values about 0.1 higher than the rural scene bands in the visible spectrum. In other spectra, except for Zone IV, the difference in fractal dimension between the two scenes reduces to about 0.05.

For the triangular prism method, the differences between the urban and rural scenes in terms of the fractal dimension values are fairly constant throughout the entire spectral range, except in Zones III and IV. Urban scene bands have values about 0.1 higher than the rural scene bands. Although not as obvious as the results from the isarithm method, the triangular prism method also gives a slightly higher contrast between the urban and rural scenes in the visible range (Zone I). Additionally, a progressive increase in $D$ values is observed within the visible light wavelength region in both the urban and rural scenes. The atmospheric scattering effect is most significant in the visible and ultraviolet regions and the scattered light tends to reduce the image contrast as well as image content. The progressive increase in the $D$ values in the visible region is probably a result of weakening of scattering effect towards the reflected infrared region. Spectral bands in the reflected infrared region (Zone II), on the other hand, capture the strongest reflectance and are not affected by the scattering effect of the atmosphere (except the noisy bands), resulting in the greatest image contrast of all spectral bands. This higher spatial complexity for the AVIRIS scenes is reflected in their slightly higher fractal dimension values in Zone II.

The declining dimension values in Figure 5b (from 2.6 to about 2.4) in Zones III and IV (i.e., bands 171 and higher) found only in the rural scene is reflected only in the triangular prism method. A closer examination of these image bands indicates that the lower dimension values are caused by two random pixels that have abnormally high spectral radiance values. These aberrant pixels cause the rest of the pixel val-

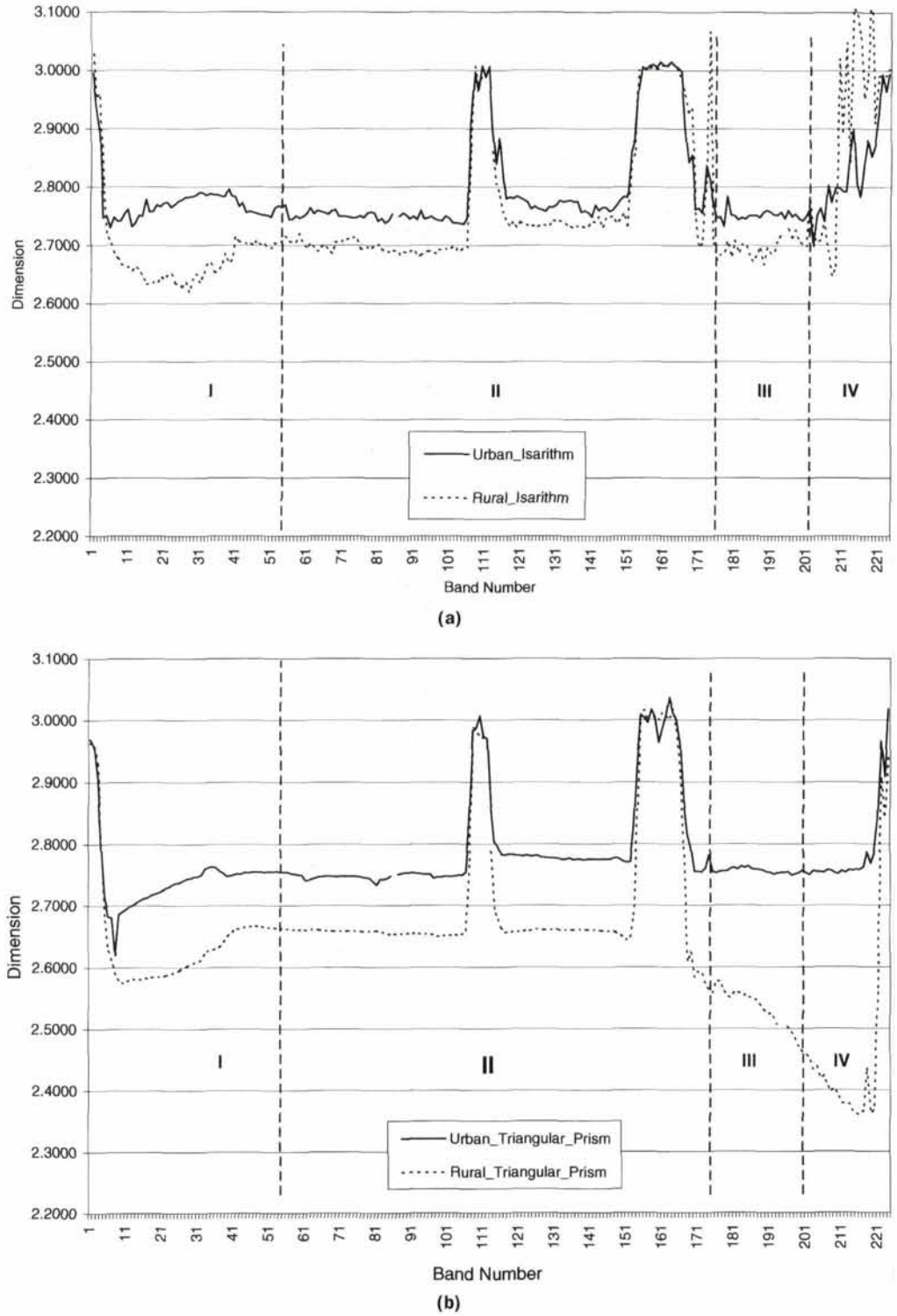


Figure 5. Graphs of fractal dimension curves for the urban scene and the rural scene computed by the isarithm (a) and triangular prism (b) methods for the two AVIRIS scenes used in this study. Notice that the urban scene has slightly higher dimension values than the rural scene for most of the spectral bands as computed by both fractal analysis methods. Roman numerals indicate the "zones" for discussing the composition of $D$ values as described in the text.

ues to be merged into a limited number of gray scales when normalization was applied to these images, making these images much smoother than they really are. This is obviously an undesirable result of the normalization process. One alternative to resolve this problem is to smooth these abnormal high pixel values before the normalization process. At the

same time, one could argue that if these pixels are "true" pixels, then the triangular prism method is able to include these extreme pixels and return a lower dimension value that accurately reflects the characteristics of the underlying surface.

The isarithm method, on the other hand, is able to exclude a few random pixels that have abnormally high values. By excluding the few number of extreme pixels, the isarithm method measures the major variation dominating the images, thereby yielding higher dimension values. This is considered an advantage, especially when dealing with remote sensing images where noisy pixels are common (Lam, 1990). However, if the few pixels that have extreme values are "true" pixels, then the isarithm method will not be able to measure the "true" surface complexity that includes the extremes.

Another observation of the dimension values given in Figures 5a and 5b is that the dimension curve of the isarithm method shows more minor variation among image bands, whereas the dimension curve derived from the triangular prism method is quite stable (except in the problem zones). The fact that the extreme pixels have almost no effect on the isarithm method supports our earlier finding that the isarithm method may be used when the goal is to measure the dominant surface variation, and, in this sense, the isarithm method is considered more robust.

Normalization of image pixel values is necessary for the triangular prism method in order to make the results comparable among all bands. Furthermore, the triangular prism method is sensitive to extreme values of the surface, albeit they are noisy pixels. When a few extreme pixels are present, the triangular prism method will yield a lower dimension value. Thus, it is important in applying the triangular prism method to remotely sensed data to first assess whether the image has any noisy pixels that will affect $D$ values.

## Conclusions

This paper compares how the spatial complexity of two AVIRIS scenes, one representing an urban and the other a rural landscape, changes across the entire spectral range of the data. Similar to the findings from previous studies on Landsat TM imagery, this study shows that, in hyperspectral imagery, urban landscapes have a higher dimension than rural landscapes (i.e., a $D$ value of approximately 0.1 or higher), and higher contrast in fractal dimension values between the two landscapes occurs in the visible bands. The traditional basic statistics such as minimum, maximum, mean, standard deviation, and coefficient of variation are not effective indicators for describing and measuring the spatial variations of hyperspectral imagery. Spatial indices such as fractal dimension, therefore, must be used in conjunction with the traditional basic statistics to indicate the spatial complexity of these data. We also see where the spectral complexity of AVIRIS data affects the measurement and interpretation of $D$ values and, ultimately, the assessment of spatial complexity of these images.

Two fractal measurement methods in the ICAMS software were applied to measure the fractal dimensions of all 224 bands in the two AVIRIS scenes. The results suggest that the isarithm method is less sensitive to a very small number of extreme pixel values, which are mostly noisy pixels, in the image surfaces. On the other hand, the triangular prism is a very stable method, provided there are no noisy, extreme pixels in the image surfaces. Normalization of pixel values for all bands is necessary for the triangular prism method to facilitate comparison among bands.

Unusually high fractal dimension values were detected in AVIRIS bands where the signal-to-noise ratios are low. These bands are the ultraviolet bands and the three water absorption zones in the reflected infrared wavelength region. Fractal dimension can, therefore, be a useful index for screening noisy bands in hyperspectral images.

Another result from this study is the concept of using the fractal dimension curves across the entire spectrum, instead of a single dimension, to characterize landscapes manifested by the hyperspectral images. The approach of using an entire curve for analysis should be more accurate than using a single dimension from individual bands. In this study, with the exception in the problem bands, the urban curve is consistently higher than the rural curve across the spectrum, and also has greater contrast across the visible spectrum. It is possible that other landscapes may exhibit high $D$ values in one spectral range, but lower values in another (such as in the thermal wavelength region). Hence, associating the shape of the dimension curve with landscape types seems to be a promising area of research in characterizing landscapes with fractals.

Moreover, we see where fractals offer significant potential to assist in both the analysis and characterization (i.e., assessment of landscape patterns and processes) of the high spatial and spectral resolution remote sensing data that will become available to the user community in the very near future. For example, the NASA Earth Observing System (EOS) suite of sensors will provide data in many different spatial and spectral formats (EOS, 1995; EOS, 1997). Application of fractal analysis methods to data from EOS sensors (e.g., Landsat 7, ASTER, MODIS) appears, at least from this analysis of AVIRIS data, to be a useful method for evaluating how landscape characteristics will be manifested at the different spatial and spectral data scales from these sensors. Thus, we believe that the measurement and analysis of landscape-scale attributes (e.g., how landscape components change as a function of sensor spatial and spectral resolution) could be more effectively and efficiently realized through fractal characterization of high spatial and spectral resolution remote sensing data sets.

## Acknowledgments

This study is partially supported by two research grants from NASA (Award numbers: NAGW-4221 and NAG5-6517). The authors would like to thank Marcos Luna of the Department of Geography and Urban Analysis at California State University, Los Angeles, and Wei Zhao of the Department of Geography and Anthropology at Louisiana State University for their assistances in image data conversion and fractal dimension computation. This is pulibication #51 of the Center for Spatial Analysis and Remote Sensing (CSARS) at California State University, Los Angeles.

## References

Clarke, K.C., 1986. Computation of the Fractal Dimension of Topographic Surfaces Using the Triangular Prism Surface Area Method, *Computers and Geosciences*, 12(5):713–722.

De Cola, L., 1989. Fractal Analysis of a Classified Landsat Scene, *Photogrammetric Engineering & Remote Sensing*, 55:601–610.

EOS, 1995. *1995 MTPE EOS Reference Handbook*, NASA EOS Project Office, Goddard Space Flight Center, Greenbelt, Maryland, 277 p.

———, 1997. *1997 MTPE EOS Data Products Handbook, Volume 1, TRMM & AM-1*, NASA EOS Project Office, Goddard Space Flight Center, Greenbelt, Maryland, 266 p.

Gamon, J., and H.-L. Qiu, (in press). Ecological Applications of Remote Sensing at Multiple Scales, (F.I. Pugnaire and F. Valladares, editors), *Handbook of Functional Plant Ecology*, Marcel Dekker, Inc., New York.

Jaggi, S.J., D.A. Quattrochi, and N.S.-N. Lam, 1993. Implementation and Operation of Three Fractal Measurement Algorithms for

Analysis of Remote Sensing Data, *Computers and Geosciences*, 19(6):745–767.

Jarvis, P.G., 1995. Scaling Processes and Problems, *Plants, Cell and Environment*, 18:1079–1089.

Lam, N.S.-N., 1990. Description and Measurement of Landsat TM Images Using Fractals, *Photogrammetric Engineering & Remote Sensing*, 56(2):187–195.

Lam, N.S.-N., and L. De Cola, 1993. *Fractals in Geography*, Prentice Hall, Englewood Cliffs, New Jersey, 308 p.

Lam, N.S.-N., H-L. Qiu, and D. A. Quattrochi, 1997. An Evaluation of Fractal Surface Measurement Methods Using ICAMS (Image Characterization and Modeling System), *Technical Papers, ACSM/ASPRS Annual Convention, Auto-Carto* 13, ASPRS and ACSM, Bethesda, Maryland, 5:377–386.

Lam, N.S.-N., D.A. Quattrochi, H.-L. Qiu, and W. Zhao, 1998. Environmental Assessment and Monitoring with Image Characterization and Modeling System Using Multiscale Remote Sensing Data, *Applied Geographic Studies*, 2(2):77–93.

Mandelbrot, B., 1975. Stochastic Models for the Earth's Relief, the Shape and the Fractal Dimension of the Coastlines, and the Numbered-area Rule for Islands, *Proc. Nat. Acad. Sci. USA*, 72(10):3825–3828.

———, 1983. *The Fractal Geometry of Nature*, W.H. Freeman and Co., New York, 468 p.

Penuelas, J., and I. Filella, 1998. Visible and Near-Infrared Reflectance Techniques for Diagnosing Plant Physiological Status, *Trends in Plant Science*, 3(4):151–156.

Quattrochi, D.A., N.S.-N. Lam, H.-L. Qiu, and W. Zhao, 1997. Image Characterization and Modeling System (ICAMS): A Geographic Information System for the Characterization and Modeling of Multiscale Remote Sensing Data, *Scale in Remote Sensing and GIS* (D.A. Quattrochi and M.F. Goodchild, editors), CRC/Lewis Publishers, Boca Raton, Florida, pp. 295–307.

Quattrochi, D.A., N.S.-N. Lam, and H.-L. Qiu, 1998. Fractal Characterization of Multitemporal Scaled Remote Sensing Data, *Scaling of Remote Sensing Data for GIS* (N. Tate and P. Atkinson, editors), John Wiley & Sons, London (submitted).

Vane, G., R.O. Green, T.G. Chrien, H.T. Enmark, E.G. Hansen, and W.M. Porter, 1993. The Airborne Visible/Infrared Imaging Spectrometer (AVIRIS), *Remote Sensing of Environment*, 44(2/3):127–143.